Water T_2 Mapping in Fatty Infiltrated Thigh Muscles of Patients With Neuromuscular Diseases Using a T_2-Prepared 3D Turbo Spin Echo With SPAIR

Sarah Schlaeger,[1,2]* Dominik Weidlich, MSc,[1] Elisabeth Klupp, MD,[2]

Federica Montagnese, MD,[3] Marcus Deschauer, MD,[4] Benedikt Schoser, MD,[3]

Sarah Bublitz, MD,[4] Stefan Ruschke, PhD,[1] Claus Zimmer, MD,[2] Ernst J. Rummeny, MD,[1]

Jan S. Kirschke, MD,[2] and Dimitrios C. Karampinos, PhD[1]

Background: Muscle water T_2 (T_{2w}) has been proposed as a biomarker to monitor disease activity and therapy effectiveness in patients with neuromuscular diseases (NMD). Multi-echo spin-echo (MESE) is known to be affected by fatty infiltration. A T_2-prepared 3D turbo spin echo (TSE) is an alternative method for T_2 mapping, but has been only applied in healthy muscles.

Purpose: To examine the performance of T_2-prepared 3D TSE in combination with spectral adiabatic inversion recovery (SPAIR) in measuring T_{2w} in fatty infiltrated muscles based on simulations and in vivo measurements in thigh muscles of patients with NMD.

Study Type: Prospective.

Subjects: One healthy volunteer, 34 NMD patients.

Field Strength/Sequence: T_2-prepared stimulated echo acquisition mode (STEAM) magnetic resonance spectroscopy (MRS), SPAIR STEAM MRS, and SPAIR T_2-prepared STEAM MRS were performed in the subcutaneous fat of a healthy volunteer's thigh. T_2 mapping based on SPAIR 2D MESE and SPAIR T_2-prepared 3D TSE was performed in the NMD patients' thigh region. Multi-TE STEAM MRS was performed for measuring a reference T_{2w} at different thigh locations.

Assessment: The behavior of the fat spectrum in the SPAIR T_2-prepared 3D TSE was simulated using Bloch simulations. The in vivo T_2 results of the imaging methods were compared to the in vivo T_{2w} MRS results.

Statistical Tests: Pearson correlation coefficient with slope and intercept, relative error.

Results: The simulated T_2 for the SPAIR T_2-prepared 3D TSE sequence remained constant within a relative error of not more than 4% up to a fat fraction of 80%. In vivo T_2 values of SPAIR T_2-prepared 3D TSE were in good agreement with the T_{2w} values of STEAM MRS (R = 0.86; slope = 1.12; intercept = –1.41 ms). In vivo T_2 values of SPAIR 2D MESE showed large deviations from the T_{2w} values of STEAM MRS (R = 0.14; slope = 0.32; intercept = 38.83 ms).

Data Conclusion: The proposed SPAIR T_2-prepared 3D TSE shows reduced sensitivity to fatty infiltration for T_{2w} mapping in the thigh muscles of NMD patients.

Level of Evidence: 1

Technical Efficacy: Stage 1

MUSCLE WATER T_2 (T_{2w}) has been proposed as an important imaging marker for pathophysiological changes of skeletal muscle tissue.[1,2] Muscle T_{2w}, in contrast to muscle global T_2, reflects the chemically selective T_2 decay of the water component in the muscle tissue and is therefore considered an indicator for water mobility in the tissue.[2,3] Water mobility in the muscle tissue is affected by several circumstances, such as inflammation, myocyte swelling, sarcoplasmic leakiness, cell necrosis, hydrostatic edema, denervation, or exercise of moderate to high intensity.[1,2] Therefore, T_{2w} is a rather unspecific parameter, although responding rapidly to alterations in the muscle tissue and allowing assessment of acute as well as chronic changes.[2,4–6] Due to its high sensitivity to alterations in the muscle fibers, T_{2w} has seen a growing consideration in the assessment of patients with neuromuscular diseases (NMD), where T_{2w} is currently considered a potential marker for diseases activity.[1,2,4,5,7] T_{2w} has been proposed as an outcome measure to monitor muscle disease status and evaluate response to treatment.[8,9]

The measurement of T_{2w} using quantitative magnetic resonance sequences allows objective, comparable, and precise assessment of even small changes in the muscle fiber composition.[2,6] Single-voxel H^1 magnetic resonance spectroscopy (MRS) is considered the reference standard for robust quantification of muscle T_{2w}, as it determines the relative concentration of water and various metabolites and can also resolve the spectral complexity of fat.[10,11] Therefore, single-voxel H^1 MRS enables a fat fraction independent quantification of T_{2w}.

In patients with NMD, pathological changes in the muscle tissue such as fatty and edematous alterations are often simultaneously present in a single muscle, affecting the muscle heterogeneously.[1] There is thus a need for techniques enabling robust and accurate spatially resolved T_{2w} quantification.[12] Thereby, especially the thigh musculature is a region of high interest for the application of quantitative imaging techniques, as it can be easily assessed with MRI due to its larger size compared to other body muscles and its relatively low B_1 and B_0 inhomogeneities.[13] The thigh typically shows diagnostically important disease characteristic patterns of muscle involvement.[14,15]

As analysis based on MRS does not contain any spatial information and spatially resolved chemical-shift imaging (CSI) can be time-consuming, prone to artifacts, and limited in spatial resolution,[16] time-efficient quantitative imaging techniques for T_2 mapping are emerging. Several challenges need to be addressed for a robust quantitative T_{2w} determination. Transmit B_1 and B_0 inhomogeneities are a well-known source of errors for T_{2w} quantification, especially in the thigh.[17–19] In the heterogeneously affected muscle tissue, the presence of fatty infiltration also affects T_{2w} estimation,[1,20–22] as a complete fat suppression is challenging due to the complexity of the fat spectrum with different chemical shift, T_1 and T_2 for each fat peak. Fatty infiltration and edematous changes both lead to increased T_2 values in the muscle tissue in most sequences. The effects of fatty infiltration and edematous changes on T_2 values cannot, in general, be thus distinguished.[23] Therefore, a reduction of the influence of fat on the T_{2w} determination is highly important in fatty infiltrated muscles.

Different T_2 mapping techniques have been developed to address the above challenges in robust muscle T_{2w} determination. 2D multi-echo spin echo (MESE) sequences have been traditionally used for muscle T_2 mapping, with known limitations, including the sensitivity to transmit B_1 inhomogeneities[19,24] and the effect of fat on T_2 quantification. In order to remove the effects of transmit B_1 inhomogeneities, extended phase graph (EPG) techniques have been recently applied on 2D MESE data to model the occurrence of stimulated echoes in the decay of the signal.[1,24] Techniques modeling the presence of fat based on Dixon MESE data[25] or based on MESE data combined with a multiexponential T_2 decay model without[10] or with the phase graph formulation[1] have been proposed to remove the effect of fat. However, the robustness of the correct T_{2w} determination decreases at moderately high and high fat fractions due to small contribution of the remaining water component to the total signal.[10]

An alternative approach to reduce the effect of B_1 inhomogeneities directly during acquisition is the use of a T_2-prepared 3D turbo spin echo (TSE) sequence consisting of an adiabatic BIR-4 radiofrequency (RF) pulse in the T_2 preparation and a 3D TSE readout combined with spectral adiabatic inversion recovery (SPAIR) fat suppression.[13,26] The modified BIR-4 T_2 preparation is a method enabling accurate and precise T_2 mapping in the presence of large B_1 and B_0 offsets. It has been shown that the T_2-prepared 3D TSE sequence allows B_1-insensitive and reproducible thigh muscle T_2 mapping in a healthy cohort. However, it remains unknown how the T_2 quantification based on the SPAIR T_2-prepared 3D TSE sequence is affected by the presence of fat.

The purpose of the present work was to investigate the performance of the T_2-prepared 3D TSE combined with SPAIR fat suppression in measuring T_{2w} in fatty infiltrated muscles.

Materials and Methods
Theoretical Background
A T_2-prepared 3D TSE sequence in combination with SPAIR for fat suppression was used as proposed by Klupp et al.[13] The pulse sequence diagram is shown in Fig. 1a. The SPAIR T_2-prepared 3D TSE consists of three main components: I) the SPAIR pulse, II) the adiabatic T_2 preparation module, and III) the 3D TSE readout.

SPECTRAL ADIABATIC INVERSION RECOVERY. A SPAIR pulse at the beginning of the sequence was used to invert the main

FIGURE 1: (a) Pulse sequence diagram of the SPAIR T_2-prepared 3D TSE including I) spectral adiabatic inversion recovery, II) T2Prep module, and III) 3D TSE with flip angle modulation readout and (b) pulse sequence diagram of the SPAIR T_2-prepared single-voxel STEAM MRS including I) spectral adiabatic inversion recovery, II) T2Prep module, and III) single-voxel STEAM MRS readout.

fat peaks (Fig. 1, I).[27] Traditionally, the energy of fat is reduced by nulling the main fat peak (methylene, at 1.3 ppm) at the beginning of the readout and reducing thereby the contribution of fat on the overall acquired signal. Keeping in mind that fat has multiple peaks with different T_1 relaxation times, SPAIR will not null all the fat peaks at once, rather than greatly reduce the total fat energy. Additionally, if off-resonance effects are neglected, SPAIR fat suppression does not affect the olefinic and glycerol fat peaks located in the spectral proximity to the water peak. After SPAIR inversion and the inversion delay time, some of the fat peaks may be nulled, some may be inverted, but reduced in energy, some may be already positively recovered, but reduced in energy, and some may not be affected at all. Keeping this complex fat signal behavior in mind, the total energy of the fat signal is expected to be smaller than weighted by simple T_1 relaxation. At the echo, the energy of the inverted and the noninverted fat peaks is summed and this can lead to additional fat signal reduction. In the present work, the inversion time between SPAIR and the beginning of the T_2 preparation module was determined experimentally in order to reduce the total fat signal at the beginning of the readout as strongly as possible. The experimental determination of the inversion delay time was optimized in one healthy volunteer by minimizing the energy in the subcutaneous fat when performing the T_2-prepared 3D TSE.

T_2 PREPARATION MODULE. The T_2 preparation module (Fig. 1, II) consists of a modified BIR-4 resonance frequency pulse with varying gaps to obtain T_2 preparation modules with different T_2 weightings.[28] Therefore, the T_2 preparation module allows a B_1-insentive T_2 weighting of the whole water-fat spectral region with at the same time equal T_1 weighting for every T_2 weighting as the T_2 preparation occurs outside of the readout. The T_2 preparation module was designed to have the final magnetization after the T_2 preparation aligned with the main magnetic field. T_1 weighting during the T_2 preparation module can be neglected due to the short duration of the T_2 preparation module.

3D TSE READOUT. The T_2 preparation module was followed by a 3D TSE readout with a flip angle modulation and appropriate start-up echoes (Fig. 1a, III). The flip angle train was designed to achieve a constant signal plateau throughout the TSE shot for

skeletal muscle tissue.[13] The TSE readout allows a very fast acquisition of the k-space center and therefore minimizes the T_1 recovery from the end of the T_2 preparation module until acquisition of the k-space center.

SIGNAL CANCELLATION OF FAT PEAKS. In the present work, it was evaluated whether the combination of the T_2-prepared 3D TSE sequence with SPAIR leads to a partial signal cancellation of fat peaks at echo acquisition. It was particularly examined whether the remaining signal of the fat peaks is relatively small compared to the signal of the water peak at the beginning of the 3D TSE readout and whether due to the relatively short maximum duration of the T_2 preparation module only minor changes of the total fat energy occur. Therefore, it was evaluated whether, after the cancellation of the fat peaks, the fat will have a small influence on the T_{2w} determination.

Simulations Based on MRS Data

In order to investigate the performance of the T_2-prepared 3D TSE sequence in combination with SPAIR on T_{2w} determination the following signal model was used:

$$Signal(T2Prep) = (1 - FF) \cdot W(T2Prep) + FF \cdot c(T2Prep) \cdot F(T2Prep) \tag{1}$$

where FF is the fat fraction, $W(T2Prep)$ the water signal, and $F(T2Prep)$ the fat signal. $F(T2Prep)$ represents the combined fat signal of all fat peaks. When the different fat peaks cancel each other out, the ratio of the fat signal contributing to the total signal in Eq. [1] is reduced. A constant $c(T2Prep)$ was introduced, representing the energy reduction factor of SPAIR due to T_1 relaxation.

In order to solve the signal model equation, the constant $c(T2Prep)$ and the combined fat signal $F(T2Prep)$ have to be determined. To accurately investigate the behavior of the different fat peaks during the different components of the SPAIR T_2-prepared 3D TSE sequence, appropriate MRS sequences were designed. In the subcutaneous fat of a healthy volunteer's thigh (female, 24 years old) a T_2-prepared stimulated echo acquisition mode (STEAM), a SPAIR STEAM, and a SPAIR T_2-prepared STEAM according to the pulse sequence diagram in Fig. 1 were performed. Figure 1b

shows the different components of the SPAIR T_2-prepared STEAM MRS sequence. The sequence parameters for the T_2-prepared STEAM, the SPAIR STEAM, and the SPAIR T_2-prepared STEAM are listed in Table 1.

Based on the acquired MRS data from the in vivo experiments in the subcutaneous fat, additional simulations were performed to calculate c(T2Prep) and F(T2Prep). Therefore, T_1 and T_2 weightings of the STEAM MRS sequence were removed mathematically based on T_1 and T_2 relaxation times extracted from a STEAM TE- and TM-Series in the subcutaneous fat of the same volunteer. A Bloch simulation of the 3D TSE readout was then performed. The simulation was implemented in MatLab (MathWorks, Natick, MA) and performed a numerical calculation of the magnetization time evolution in discrete time steps based on the well-known Bloch equation.[29]

Based on the simulated fat peak area the constant c (T2Prep) and the remaining combined fat signal F(T2Prep) were calculated.

Using the experimental data from the MRS measurements in the subcutaneous fat of a healthy volunteer's thigh and the signal model presented in Eq. [1], different signal decay curves for the water and fat signal components were determined. The total signal, Signal(T2Prep), which represents the T_2 signal of the SPAIR T_2-prepared 3D TSE imaging sequence, was calculated using Eq. [1]. For different fat fractions, different Signal(T2Prep) values were calculated and T_2 was estimated by fitting Signal(T2Prep) to a single-exponential T_2 signal expression.

In Vivo MR Measurements in NMD Patients

The study was approved by the local Ethics Commission and written informed consent was obtained from all patients before participation. In order to verify the fatty infiltration independent determination of T_{2w} using the SPAIR T_2-prepared 3D TSE, MR measurements were performed in the thigh of 34 patients (64.7% women) with different NMD (Table 2) with a 3 T system (Ingenia, Philips Healthcare, Best, The Netherlands). The whole-body coil, the built-in 12-channel posterior coil, and a 16-channel anterior coil were used. The 16-channel anterior coil was placed on top of the hip and thigh region. Subjects were positioned in a head-first supine position.

Spatially-resolved PDFF mapping was performed for a reference using a six-echo 3D spoiled gradient echo sequence with bipolar readouts. In order to calculated T_2 maps, a 2D MESE with SPAIR fat suppression and a T_2-prepared 3D TSE with SPAIR fat suppression were acquired in one stack in the mid-thigh. A multi-TE single-voxel STEAM MRS was performed in multiple locations by moving the MRS box within the patients' healthy, edematous, and fatty thigh muscles. The thigh muscles where MRS was applied were selected by qualitative assessment by the scanner operator based on the T_2-weighted water- and fat-separated images of a T_2-weighted Dixon TSE sequence and varied depending on the patients' muscle disease pattern.[30] The sequence parameters for SPAIR 2D MESE, SPAIR T_2-prepared 3D TSE, multi-TE single-voxel STEAM MRS, the T_2-weighted Dixon TSE, and the six-echo 3D spoiled gradient echo sequence are shown in Table 3. The longest duration of the T_2 preparation module in the present work was 60 ms, resulting in an effective T_2 weighting of 56.9 ms and verifying the assumption of neglectable T_1 weighting during the T_2 preparation module.[31] The parameters of the employed BIR-4 RF pulse were: total pulse duration without gaps of the T_2 preparation module = 10 ms, B_1 amplitude = 13.5 μT, and frequency sweep = 3700 Hz. The parameters for the employed SPAIR pulse were: pulse duration = 18.4 ms, B_1 amplitude = 7.3 μT, pulse bandwidth = 680 Hz.

TABLE 1. Sequence Parameters of T_2-Prepared STEAM MRS, SPAIR STEAM MRS, and SPAIR T_2-Prepared STEAM MRS Performed in a Healthy Volunteer

	T_2-prepared STEAM MRS	SPAIR STEAM MRS	SPAIR T_2-prepared STEAM MRS
VOI (mm^3)	15 x 15 x 15	15 x 15 x 15	15 x 15 x 15
Spectral BW (Hz)	5000	5000	5000
Flip angle (deg)	90	90	90
TR (ms)	2000	2000	2000
TE (ms)	21	20/30/40/50/60	21
TM (ms)	16	16	16
Fat suppression	—	SPAIR, inversion delay 205 ms	SPAIR, inversion delay 205 ms
Startup acquisitions	1	1	1
NSA	24	24	24
Phase cycles	8	8	8
T_2 prepartion durations (ms)	20/30/40/50/60	—	20/30/40/50/60
Scan duration (min)	04:10	04:10	04:10

TABLE 2. Patient ID, Age, Gender, and Disease of 34 Patients With NMD

Patient ID	Age	Gender	Disease
P001	63	F	Myotonic dystrophy type 2
P002	54	F	Myotonic dystrophy type 2
P003	47	F	Limb girdle muscular dystrophy type 2A
P004	34	F	Myotonic dystrophy type 2
P005	49	F	Limb girdle muscular dystrophy type 2A
P006	30	F	Limb girdle muscular dystrophy type 2I
P007	26	M	Limb girdle muscular dystrophy type 2A
P008	61	F	Myotonic dystrophy type 2
P009	52	M	Myotonic dystrophy type 2
P010	45	M	Centronuclear myopathy
P011	52	F	Limb girdle muscular dystrophy type 2A
P012	41	M	Amyotrophic lateral sclerosis
P013	61	M	Unclassified myopathy
P014	50	F	Unclassified myopathy
P015	45	F	Limb girdle muscular dystrophy type 2A
P016	19	F	Inflammatory myopathy
P017	20	F	Lamin A/C myopathy
P018	77	M	Inclusion body myositis
P019	22	F	Facioscapulohumeral muscular dystrophy
P020	57	M	Nemaline myopathy 2
P021	66	F	Myotonic dystrophy type 2
P022	36	F	Dermatomyositis
P023	26	F	Rhabdomyolysis
P024	49	F	Bethlem myopathy
P025	55	M	Amyotrophic lateral sclerosis
P026	32	F	Myotonic dystrophy type 1
P027	76	F	Pompe disease
P028	84	M	Pompe disease
P029	70	M	Hypokalemic periodic paralysis

TABLE 2. Continued

Patient ID	Age	Gender	Disease
P030	34	F	Distal myopathy
P031	73	F	Myofibrillar myopathy
P032	69	F	Inclusion body myositis
P033	41	M	Dermatomyositis
P034	48	M	Limb girdle muscular dystrophy type 2L

Data Analysis

PROCESSING OF MRS DATA. The processing of the MRS data was performed with in-house software and included zero-order phasing, Gaussian apodization, and frequency alignment of single acquisitions. For the MRS scan in the health volunteer's subcutaneous fat, the peak area quantification was performed considering six fat peaks and fitting of the fat peak areas was performed independently for each echo time (TE). No more than six fat peaks were considered for the analysis because an accurate determination of T_1 and T_2 relaxation constants as well as peak amplitudes after inversion recovery was only possible when the initial energy of the fat peak was sufficiently high. For the MRS scans performed in the patients with NMD, eight to ten fat peaks (depending on the fat fraction and therefore visibility of smaller fat peaks)[32] were considered and the measurement of all four/five TEs was jointly incorporated into a peak-specific T_2 decay signal model.[33] Fitting was constrained with a common fat T_2 (T_{2f}) for all fat peaks. Based on the fat and water T_2 as well as the fat peak amplitudes, the proton density fat fraction (PDFF) was calculated. The MRS quantification was eventually utilized to extract both PDFF and T_{2w}. The MRS-based PDFF values were used in the subsequent statistical analysis.

PROCESSING OF IMAGING DATA. The processing of the multiecho gradient echo data was performed online using the vendor's routines for PDFF mapping. After phase error correction, water-fat separation was performed based on a complex-based signal formulation employing a multipeak fat spectrum and single T_2^* decay correction.[34,35] A small flip angle was used to minimize T_1 bias effects.[36] The imaging-based PDFF maps were only used for visualizing the spatially heterogeneous muscle fatty infiltration patterns.

Postprocessing of the T_2 maps was performed offline. An exponential fit with linear least-squares was used to fit data. For the MESE data the first echo was excluded to reduce T_2 overestimation due to stimulated echoes.

STATISTICAL ANALYSIS PERFORMED IN NMD PATIENTS. The statistical analyses were performed using MatLab. Measured T_2 values of the SPAIR 2D MESE sequence and the SPAIR T_2-prepared 3D TSE sequence were correlated with T_{2w} values determined by STEAM MRS using the Pearson correlation coefficient R. Intercept and slope were determined. The relative error of the T_2

TABLE 3. Sequence Parameters of SPAIR 2D MESE, SPAIR T_2-prepared 3D TSE, Multi-TE Single-Voxel STEAM MRS, T_2-weighted Dixon TSE and Six-echo 3D Spoiled Gradient Echo Sequence for PDFF Mapping, Performed in NMD Patients

	SPAIR 2D MESE	SPAIR T_2-prepared 3D TSE	Multi-TE single-voxel STEAM MRS	T_2W Dixon TSE	Six-echo 3D spoiled gradient echo sequence
TR (ms)	2200	1500	6000	3725	10
TE (ms)	10 echoes with $TE_1 = 20$	19	11/15/20/25(/35) with 8 averages	100	1.17
ΔTE (ms)	10	—	—	1.0	0.9
TM (ms)	—	—	16	—	—
Number of slices	30	30	—	26	30
Slice gap (mm)	0	0	—	6	0
Acquisition voxel (mm^3)	2 x 2 x 4	2 x 2 x 8	15 x 15 x 15	2.5 x 2.7 x 6.0	3.2 x 2 x 4
T_2 prepartion durations (ms)	—	20/30/40/50/60	—	—	—
RF-pulses (in readout)	180° refocusing pulses	Flip angle modulated TSE readout (echo spacing: 2.4 ms, 5 start-up echoes)	Slice selective 90° excitation pulses	—	Flip angle of 3°
TSE factor	—	50	—	45	—
Averages	1	Partial averaging (1.4)	8 (4 phase cycles)	2	1
FOV/VOI (mm^3)	420 x 260 x 120	420 x 260 x 120	15 x 15 x 15	330 x 450 x 306	260 x 420 x 120
Scan duration	8:24 min	4:30 min	3:36 (4:30) min	2:07 min	0:20
SENSE	In A/P direction, reduction factor 2	In A/P direction, reduction factor 2	—	—	In L/R direction, reduction factor 2

values of the SPAIR 2D MESE sequence and the SPAIR T_2-prepared 3D TSE sequence compared to the T_{2w} values determined by STEAM MRS was calculated in correlation with MRS-based PDFF.

Results

Healthy Volunteer MRS Results

Figure 2 shows the spectra of the multi-TE single-voxel STEAM MRS performed in the subcutaneous fat of a healthy volunteer's thigh. The spectrum of the T_2-prepared STEAM (Fig. 2a) shows a conventional fat spectrum. The different T_2 weightings that reduce the amplitude of the fat peaks can be observed. In the SPAIR STEAM spectrum (Fig. 2b), the total fat energy is largely reduced. The total fat energy reduction is best visible when referencing the fat peak signals in Fig. 2a and Fig. 2b to the olefinic fat peaks. Furthermore, an

additional energy reduction when all the fat peaks of the spectrum are summed up can be observed. The spectrum of the SPAIR T_2-prepared STEAM (Fig. 2c) adds T_2 weighting to the SPAIR STEAM spectrum. The SPAIR T_2-prepared STEAM represents the fat spectrum present at the acquisition of k-space center when the SPAIR T_2-prepared 3D TSE imaging sequence is performed.

Simulation Results

Figure 3a shows the signal decay curves for the water signal (blue), for the fat signal without fat suppression (green), and for the fat signal with SPAIR fat suppression (red) in a theoretical voxel with FF = 50%. The SPAIR T_2-prepared 3D TSE imaging sequence provides the sum of the signal of the water peak and the signal of the fat peak with SPAIR fat suppression. Summing up the water signal decay curve and the
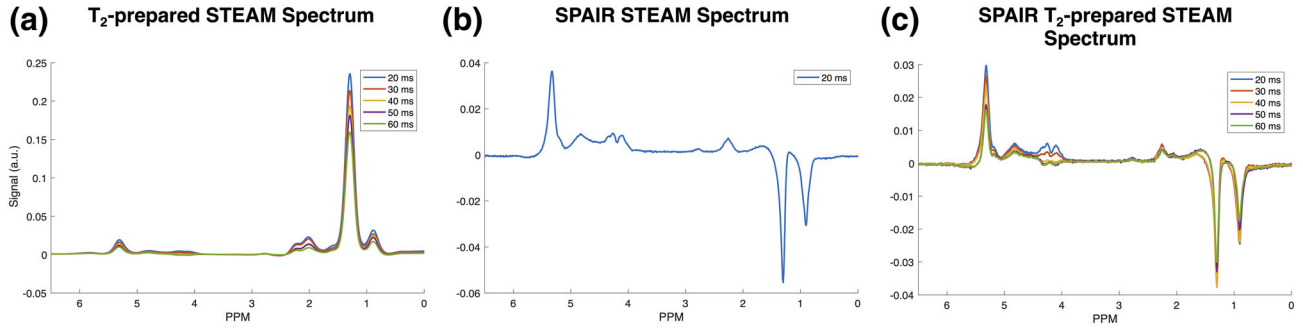
(a) T_2-prepared STEAM Spectrum

(b) SPAIR STEAM Spectrum

(c) SPAIR T_2-prepared STEAM Spectrum

FIGURE 2: Spectra of single-voxel STEAM MRS performed in the subcutaneous fat of a healthy volunteer's thigh: (a) T_2-prepared STEAM spectrum at different echo times, (b) SPAIR STEAM spectrum at TE = 20 ms, and (c) SPAIR T_2-prepared STEAM spectrum at different echo times.

fat signal with SPAIR decay curve, the signal decay is largely dominated by the water signal decay. Even in a theoretical voxel with higher fat fraction, such as FF = 75%, the summed up signal decay of the imaging is largely dominated by the water signal decay and the influence of the fat signal with SPAIR stays small (Fig. 3b).

Based on the results of the MRS measurements in the subcutaneous fat and the Bloch simulations, the following parameters with their dependency on the duration of the T_2 preparation module were determined: $c(T2Prep)$ = [0.22 0.21 0.21 0.20 0.19] and $F(T2Prep)$ = [0.12 0.08 0.04 0.05 0.04] for the T_2Prep durations of [20 30 40 50 60] ms. Figure 3c shows the dependence of the simulated T_2 on different fat fractions. The simulated T_2 remains constant within a relative error of not more than 4% up to a fat fraction of 80%. At fat fraction values higher than 80%, deviations from the nominal T_2 values can be observed.

NMD Patients in vivo Results

Representative PDFF maps and T_2 maps based on the SPAIR 2D MESE sequence and the SPAIR T_2-prepared 3D TSE sequence of the thigh of a patient with Pompe disease are shown in Fig. 4. The patient has highly fatty infiltrated muscles, partially fatty infiltrated muscles, and muscles without fatty infiltration. The red arrow indicates T_2 elevations in the SPAIR 2D MESE in contrast to a stable T_2 in the SPAIR T_2-prepared 3D TSE in a region which is typically affected by B_1 errors. In a moderately fatty infiltrated region (PDFF = $25.6 \pm 14.5\%$ – circle), the mean T_2 value of the SPAIR 2D MESE was 54.6 ± 11.8 ms, whereas the mean T_2 value of the SPAIR T_2-prepared 3D TSE was 35.4 ± 3.8 ms.

Figure 5 shows the results of the comparison of T_{2w} values determined by STEAM MRS and T_2 mapping data in the scanned 34 NMD patients based on measurements in fatty infiltrated muscle tissue, edematous muscle tissue, and healthy muscle tissue locations. A good agreement between T_{2w} values of STEAM MRS and T_2 values of SPAIR T_2-prepared 3D TSE is reported (R = 0.86; $P < 10^{-3}$; slope = 1.12; intercept = -1.41 ms), whereas the T_2 values of SPAIR 2D MESE show

(a) Signal Decay in Voxel with 50% Fat Fraction

(b) Signal Decay in Voxel with 75% Fat Fraction
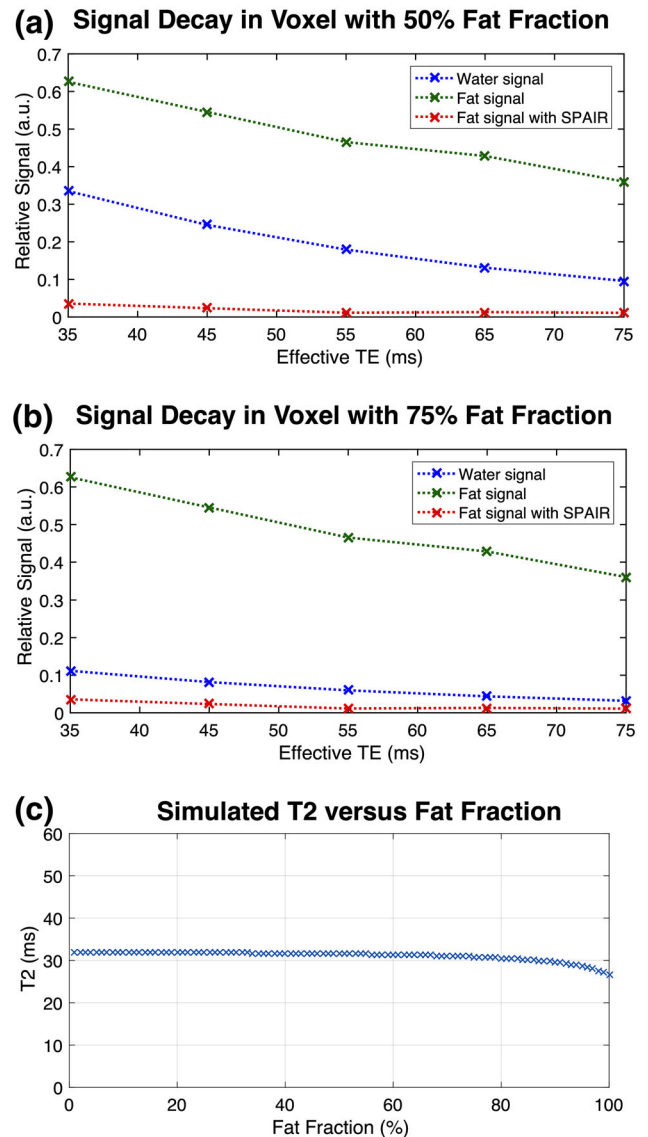
(c) Simulated T2 versus Fat Fraction

FIGURE 3: (a,b) Simulated SPAIR T_2-prepared T_2-weighted signal decay curves as a function of effective TE for the water signal (blue), the fat signal without fat suppression (green), and the fat signal with SPAIR fat suppression (red) for (a) a voxel with 50% fat fraction and (b) a voxel with 75% fat fraction. (c) Simulated estimated T_2 vs. fat fraction. The simulated T_2 stays rather constant up to a fat fraction of 80%.
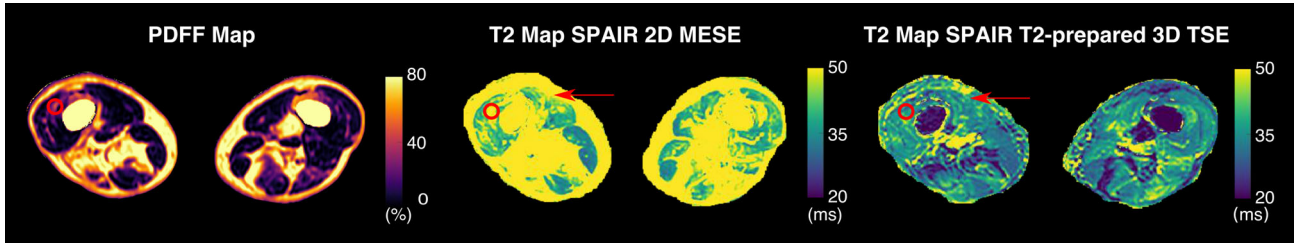
FIGURE 4: Representative PDFF map, T_2 map using SPAIR 2D MESE and T_2 map using SPAIR T_2-prepared 3D TSE in a patient with Pompe disease. The red arrow indicates a region of typical B_1 inhomogeneity and the red circle indicates a region of moderate fatty infiltration.

large deviations from the T_{2w} values of STEAM MRS ($R = 0.14$; $P < 10^{-3}$; slope = 0.32; intercept = 38.83 ms). The relative error in the T_2 measurement using the SPAIR T_2-prepared 3D TSE was below 25%, even at PDFF values larger than 60%. The relative error in the T_2 measurement using the SPAIR 2D MESE showed a strong dependence on PDFF and it exceeded 100% at PDFF values larger than 60%.

Discussion

The present work examines how T_{2w} quantification based on the T_2-prepared 3D TSE sequence with SPAIR fat suppression is affected by the presence of fatty infiltration in skeletal muscle. Therefore, simulations were performed based on MRS measurements in the subcutaneous fat of a healthy volunteer's thigh to theoretically assess the T_2 quantification accuracy of the SPAIR T_2-prepared 3D TSE in the presence of fat. Additionally, SPAIR T_2-prepared 3D TSE T_2

measurements were performed in the fatty infiltrated thigh region of 34 patients with various NMD and compared to the routinely used SPAIR 2D MESE T_2 measurements, using single-voxel MRS T_{2w} measurements as the reference standard.

The combination of MESE with fat suppression techniques is known to result in T_2 values in fatty infiltrated skeletal muscles still affected by the presence of fat.[37] The reported simulations based on measurements in the subcutaneous fat of a healthy volunteer's thigh confirm the theory that the T_2-prepared 3D TSE in combination with SPAIR leads to a partial signal cancellation of fat peaks at echo acquisition, enabling a robust determination of T_{2w} values with only a small influence of the remaining fat signal. The relative independence of T_{2w} determination on the underlying fat fraction is mainly due to 1) the partial signal cancellation of the fat peaks caused by the signal reduction of the fat peaks
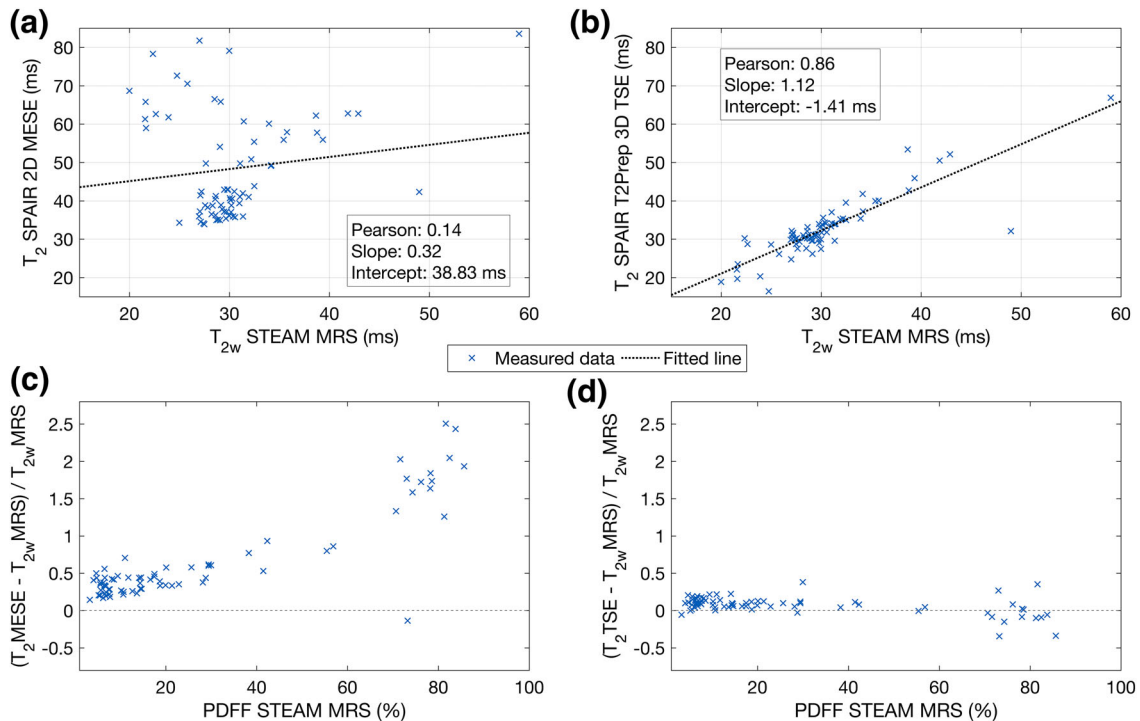

FIGURE 5: (a) T_2 from SPAIR 2D MESE vs. T_{2w} from STEAM MRS and (b) T_2 from SPAIR T_2-prepared 3D TSE vs. T_{2w} from STEAM MRS. (c) Relative error of SPAIR 2D MESE compared to T_{2w} from STEAM MRS as a function of PDFF and (d) relative error of SPAIR T_2-prepared 3D TSE compared to T_{2w} from STEAM MRS as a function of PDFF. Results show data from 34 NMD patients.

by the SPAIR inversion pulse; 2) the equal fat T_1 weighting for every T_2 weighting during the T_2 preparation module; and 3) the 3D TSE readout enabling the fast acquisition of the *k*-space center and therefore minimizing any fat T_1 recovery effects.

The reported in vivo results show that T_{2w} mapping based on SPAIR T_2-prepared 3D TSE is minimally sensitive to fatty infiltration even at higher PDFF values, and approximately reveals the same T_{2w} values as the reference standard MRS. To the best of the authors' knowledge, the present work is the first to compare quantitative spatially-resolved imaging data based on T_2 maps with MRS in a large number of patients with NMD. Robust T_{2w} mapping, which is comparable to MRS as a reference standard, is essential to get an insight into the spatial distribution of acute and chronic alterations and disease activity in the muscle tissue of patients with NMD.[3,12] A robust and fat independent determination of the important biomarker T_{2w} is essential, especially in NMD patients, as regions with healthy muscle tissue, edematous muscle tissue, and fatty infiltrated muscle tissue are often simultaneously present in a single muscle of NMD patients.

Previous works have addressed the confounding effects of transmit B_1 sensitivity and fat on T_{2w} quantification in MESE sequences by appropriate signal modeling of the relevant effects, primarily using EPG formulations.[1,10] T_{2w} mapping based on the T_2-prepared 3D TSE has been previously shown to be insensitive to transmit B_1 inhomogeneity effects in the thigh muscles[13] and the present work shows that with the addition of SPAIR on the T_2-prepared 3D TSE, the effect of fat on the measured thigh muscle T_2 is also minimized. Therefore, the present SPAIR T_2-prepared 3D TSE sequence effectively and simultaneously addresses the confounding effects of transmit B_1 sensitivity and fat on T_{2w} quantification already on the acquisition side and thus does not rely on modeling of the above two effects on the signal evolution (as performed in MESE acquisitions.[1,10])

Limitations

The present work has some limitations. First, the present approach for fatty infiltration independent determination of T_{2w} in muscle tissue based on SPAIR is specific to the employed T_2-prepared 3D TSE imaging protocol and cannot be necessarily generalized to other T_2 mapping techniques. Second, the measured T_{2w} using the SPAIR T_2-prepared 3D TSE remains an approximation of the T_{2w} value, as the signal of the different fat peaks is not completely suppressed or separated, and rather the effect of unsuppressed fat is reduced. Third, although the performance of the T_2-prepared 3D TSE is quite independent of transmit B_1 and B_0 field inhomogeneities, the performed SPAIR preparation is prone to B_0 inhomogeneity effects. The sensitivity of SPAIR to B_0 inhomogeneity effects can affect the effectiveness of the inversion of the main fat peaks.[27] However, the effect of B_0

inhomogeneities on the SPAIR pulse is estimated to be small, at least for thigh muscle imaging at 3 T. Concerning study design limitations, fourth, the present simulations in order to explain the performance of the combination of SPAIR with the T_2-prepared 3D TSE in regions of fatty infiltrated thigh muscles are based on measurements in the subcutaneous fat of a single healthy volunteer. However, the measurements in the subcutaneous fat are only used to explain the findings of robust T_{2w} mapping with sufficient fat suppression, which is confirmed in 34 patients in the present study. Fifth, the total number of patients per each different disease group in the present study is rather small. However, the present study was performed in patients with rare diseases, and therefore the results in a small cohort number can add significant value to progress in diagnostics and therapy of NMD. Despite the small numbers per disease group, the moderate total number of patients ($n = 34$) shows the effectiveness of the proposed method for effectively measuring T_{2w} across different fatty infiltration patterns in muscle tissue.

Conclusion

T_2-prepared 3D TSE in combination with SPAIR is proposed for T_{2w} mapping in NMD patients. T_{2w} mapping using the proposed SPAIR T_2-prepared 3D TSE is known to have insensitivity to B_1 inhomogeneities and is shown as being minimally affected by the underlying fatty infiltration in thigh muscle imaging at 3 T. Therefore, the SPAIR T_2-prepared 3D TSE enables T_{2w} determination already during acquisition without the need to model the effects of B_1 inhomogeneity and fat presence. The application of the method in NMD patients shows that T_{2w} is spatially heterogeneous and the spatial resolution of T_{2w} mapping needs to be particularly considered in order to potentially monitor disease activity or therapy effectiveness in NMD patients.

References

1. Marty B, Baudin P-Y, Reyngoudt H, et al. Simultaneous muscle water T2 and fat fraction mapping using transverse relaxometry with stimulated echo compensation. NMR Biomed 2016;29:431–443.

2. Carlier PG. Global T2 versus water T2 in NMR imaging of fatty infiltrated muscles: Different methodology, different information and different implications. Neuromuscul Disord 2014;24:390–392.

3. Carlier PG, Marty B, Scheidegger O, et al. Skeletal muscle quantitative nuclear magnetic resonance imaging and spectroscopy as an outcome measure for clinical trials. J Neuromuscul Dis 2016;3:1–28.

4. Arpan I, Forbes SC, Lott DJ, et al. T2 mapping provides multiple approaches for the characterization of muscle involvement in neuromuscular diseases: A cross-sectional study of lower leg muscles in 5–15-year-old boys with Duchenne muscular dystrophy. NMR Biomed 2013;26:320–328.

5. Wary C, Azzabou N, Giraudeau C, et al. Quantitative NMRI and NMRS identify augmented disease progression after loss of ambulation in forearms of boys with Duchenne muscular dystrophy. NMR Biomed 2015;28:1150–1162.

6. English AE, Joy ML, Henkelman RM. Pulsed NMR relaxometry of striated muscle fibers. Magn Reson Med 1991;21:264–281.

7. Kim HK, Laor T, Horn PS, et al. T2 mapping in Duchenne muscular dystrophy: Distribution of disease activity and correlation with clinical assessments. Radiology 2010;255:899–908.

8. Carlier PG, Azzabou N, de Sousa PL, et al. Skeletal muscle quantitative nuclear magnetic resonance imaging follow-up of adult Pompe patients. J Inherit Metab Dis 2015;38:565–572.

9. Hollingsworth KG, de Sousa PL, Straub V, et al. Towards harmonization of protocols for MRI outcome measures in skeletal muscle studies: Consensus recommendations from two TREAT-NMD NMR workshops, 2 May 2010, Stockholm, Sweden, 1-2 October 2009, Paris, France. Neuromuscul Disord 2012;22(Suppl 2):S54–67.

10. Azzabou N, Loureiro de Sousa P, Caldas E, et al. Validation of a generic approach to muscle water T2 determination at 3T in fat-infiltrated skeletal muscle. J Magn Reson Imaging 2015;41:645–653.

11. Schlaeger S, Weidlich D, Klupp E, et al. Decreased water T2 in fatty infiltrated skeletal muscles of patients with neuromuscular diseases. NMR Biomed 2019;32:e4111.

12. Poliachik SL, Friedman SD, Carter GT, et al. Skeletal muscle edema in muscular dystrophy: Clinical and diagnostic implications. Phys Med Rehabil Clin N Am 2012;23:107–122, xi.

13. Klupp E, Weidlich D, Schlaeger S, et al. B1-insensitive T2 mapping of healthy thigh muscles using a T2-prepared 3D TSE sequence. PLoS One 2017;12:e0171337.

14. Wattjes MP, Kley RA, Fischer D. Neuromuscular imaging in inherited muscle diseases. Eur Radiol 2010;20:2447–2460.

15. Mercuri E, Clements E, Offiah A, et al. Muscle magnetic resonance imaging involvement in muscular dystrophies with rigidity of the spine. Ann Neurol 2010;67:201–208.

16. Brink HF, Buschmann MD, Rosen BR. NMR chemical shift imaging. Comput Med Imaging Graph 1989;13:93–104.

17. Crawley AP, Henkelman RM. Errors in T2 estimation using multislice multiple-echo imaging. Magn Reson Med 1987;4:34–47.

18. Majumdar S, Orphanoudakis SC, Gmitro A, et al. Errors in the measurements of T2 using multiple-echo MRI techniques. I. Effects of radiofrequency pulse imperfections. Magn Reson Med 1986;3:397–417.

19. Poon CS, Henkelman RM. Practical T2 quantitation for clinical applications. J Magn Reson Imaging 1992;2:541–553.

20. Garrood P, Hollingsworth KG, Eagle M, et al. MR imaging in Duchenne muscular dystrophy: Quantification of T1-weighted signal, contrast uptake, and the effects of exercise. J Magn Reson Imaging 2009;30:1130–1138.

21. Phoenix J, Betal D, Roberts N, et al. Objective quantification of muscle and fat in human dystrophic muscle by magnetic resonance image analysis. Muscle Nerve 1996;19:302–310.

22. Huang Y, Majumdar S, Genant HK, et al. Quantitative MR relaxometry study of muscle composition and function in Duchenne muscular dystrophy. J Magn Reson Imaging 1994;4:59–64.

23. Gold GE, Han E, Stainsby J, et al. Musculoskeletal MRI at 3.0 T: Relaxation times and image contrast. AJR Am J Roentgenol 2004;183:343–351.

24. Lebel RM, Wilman AH. Transverse relaxometry with stimulated echo compensation. Magn Reson Med 2010;64:1005–1014.

25. Janiczek RL, Gambarota G, Sinclair CD, et al. Simultaneous T(2) and lipid quantitation using IDEAL-CPMG. Magn Reson Med 2011;66:1293–1302.

26. Weidlich D, Schlaeger S, Kooijman H, et al. T2 mapping with magnetization-prepared 3D TSE based on a modified BIR-4 T2 preparation. NMR Biomed 2017;30:e3773.

27. Rosenfeld D, Panfil SL, Zur Y. Design of adiabatic pulses for fat-suppression using analytic solutions of the Bloch equation. Magn Reson Med 1997;37:793–801.

28. Haase A. Snapshot FLASH MRI. Applications to T1, T2, and chemical-shift imaging. Magn Reson Med 1990;13:77–89.

29. Bloch F. Nuclear induction. Phys Rev 1946;70:460–474.

30. Schlaeger S, Klupp E, Weidlich D, et al. T2-weighted Dixon turbo spin echo for accelerated simultaneous grading of whole-body skeletal muscle fat infiltration and edema in patients with neuromuscular diseases. J Comput Assist Tomogr 2018;42:574–579.

31. Wang G, El-Sharkawy AM, Edelstein WA, et al. Measuring T2 and T1, and imaging T2 without spin echoes. J Magn Reson 2012;214:273–280.

32. Ruschke S, Kienberger H, Baum T, et al. Diffusion-weighted stimulated echo acquisition mode (DW-STEAM) MR spectroscopy to measure fat unsaturation in regions with low proton-density fat fraction. Magn Reson Med 2016;75:32–41.

33. Dieckmeyer M, Ruschke S, Cordes C, et al. The need for T(2) correction on MRS-based vertebral bone marrow fat quantification: Implications for bone marrow fat fraction age dependence. NMR Biomed 2015;28:432–439.

34. Yu H, Shimakawa A, McKenzie CA, et al. Multiecho water-fat separation and simultaneous R2* estimation with multifrequency fat spectrum modeling. Magn Reson Med 2008;60:1122–1134.

35. Yu H, McKenzie CA, Shimakawa A, et al. Multiecho reconstruction for simultaneous water-fat decomposition and T2* estimation. J Magn Reson Imaging 2007;26:1153–1161.

36. Karampinos DC, Yu H, Shimakawa A, et al. T(1)-corrected fat quantitation using chemical shift-based water/fat separation: Application to skeletal muscle. Magn Reson Med 2011;66:1312–1326.

37. Wokke BH, Van Den Bergen JC, Hooijmans MT, et al. T2 relaxation times are increased in skeletal muscle of DMD but not BMD patients. Muscle Nerve 2016;53:38–43.